Nonlinear MPC for combined motion control and thrust allocation of ships

For future autonomous marine vessels, better understanding of the ship's behavior and control performance will be essential.

ALEXANDER BÄRLUND
ABB Corporate Research

JONAS LINDER
Senior Scientist
ABB Corporate Research

HAMID REZA FEYZMAHDAVIAN
Senior Scientist
ABB Corporate Research

MICHAEL LUNDH
Senior Principal Scientist
ABB Corporate Research

KALEVI TERVO
Corporate Executive Engineer and Global Program Manager
ABB Marine & Ports

Traditional motion control systems for ships decouple the problem into high-level motion control of the ship and thrust allocation to achieve the desired control action through the available actuators. The benefit is a segmented software, aiding in development and commissioning. The drawback of this decoupling is that the high-level controller at best has an approximate model of the capabilities in the thruster system. This typically leads to a mismatch between desired and achieved force especially when the control becomes aggressive.

In this paper, a model predictive controller is proposed to solve both tasks simultaneously and overcome this drawback. The controller is based on a low-speed ship and thruster model and the resulting optimization problem is solved using the ACADO toolkit. A simulation study of a supply vessel with only two thrusters is presented to investigate the behavior of the proposed controller in aggressive low speed maneuvering. The results show that there are benefits to incorporating the proposed controller.

When it comes to autonomous vessels, motion control is a task of particular interest. It deals with the design of control laws that allow the ship to perform specific tasks, such as keeping a position and heading angle, tracking way-points, or following desired paths.

For low speed, the motion control system (MCS) is generally decoupled into a high-level controller, which computes forces, and torque to be exerted on the ship and thrust allocation (TA), which is responsible for distributing the control effort among available actuators (Sørrensen, 2011).

Design of high-level controllers for marine vessels have been widely studied in the literature using different approaches ranging from PID to nonlinear controllers (Fossen, 2011). One important aspect is to explicitly account for physical constraints on forces and torques generated by ship actuators. In general, either such constraints are completely neglected, or the controller is specially tuned so that they are not violated under desired conditions.

One of the few techniques in the literature which is capable of handling constraints is model predictive control (MPC). An early MPC application for marine vessels is Wahl and Gilles (1998), where rudder saturation was considered in the control design. The use of MPC has been recently explored for dynamic positioning (Hvamb, 2001; Sotnikova and Veremey, 2013), trajectory tracking (Zheng et al., 2014), and path following of marine vessels (Li et al., 2009).

In applications where TA is used, vessels are commonly over-actuated. The TA is usually formulated as a constrained optimization problem which search for the best solution within physical limitations on actuators, while minimizing some user-defined criterion, for example, consumed power. To achieve better performance, a recent advance is towards MPC-based TA algorithms. This allows the algorithm to optimize rate limited states in the long run, to reduce the power consumption as well as reducing the environmental disturbances in the thruster commands (Skjong and Pedersen, 2017).

This decoupled approach offers the advantage of a modular design where the high-level controller can be designed without detailed knowledge about the vessel's actuator configuration (Johansen and Fossen, 2013). However, this also implies that the generalized force command does not consider the physical limitations of the thruster system, such as limited rotation rate of azimuth thrusters and asymmetric efficiency. This typically give a mismatch between commanded and desired force. To counteract this problem, Veksler et al. (2016) combined the high-level controller and TA into one MPC algorithm to achieve optimal control of the thrusters for a DP application.

In this work, similarly to Veksler et al. (2016), a single MPC controller is used. However, here, the focus is on transient behavior and velocities close to the boundary of low-speed motion control rather than the DP application. Moreover, the applications of interest are vessels that have fewer actuators than a typical DP vessel. Examples of applications could be automated approaches for cruise vessels or low-speed path following for ferries.

Ship model

The notation in this paper will be adopted from Fossen (2011). Here, the ship model is only summarized, for details, the interested reader is referred to Fossen (2011) or Perez (2005) and references therein.

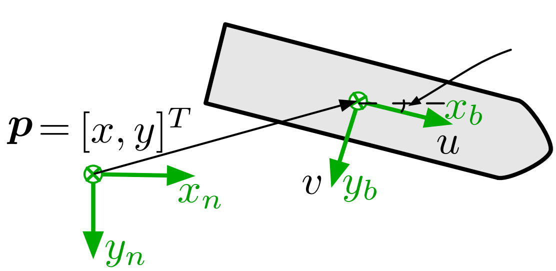

Figure 1: Definition of coordinate systems and velocities

Ship dynamics

This paper regards controlling the position and heading of a ship on the ocean surface at low speed and only the horizontal 3 degrees of freedom (DOF) motion will be considered. The motion of the ship is described using two coordinate systems, a body-fixed system, which is attached to the ship and an Earth-fixed system, which is assumed to be inertial, see Figure 1. The body-fixed generalized velocity is described by $\boldsymbol{\nu} = [u\ v\ r]^T$ and the Earth-fixed generalized position is described by $\boldsymbol{\eta} = [x\ y\ \psi]^T$. Here, u is the surge velocity, v is the sway velocity, r is the yaw velocity, x and y is the position in a North-East-Down (NED) coordinate system and ψ is the heading. The relationship between the velocity and the position is purely geometric and is described by

$$\dot{\boldsymbol{\eta}} = \boldsymbol{R}(\psi)\boldsymbol{\nu} \tag{1}$$

where the rotation matrix is given by

$$\boldsymbol{R}(\psi) = \begin{bmatrix} \cos\psi & -\sin\psi & 0 \\ \sin\psi & \cos\psi & 0 \\ 0 & 0 & 1 \end{bmatrix} \tag{2}$$

A model of the kinetic motion for ships can be derived using rigid-body mechanics and theory of hydrodynamics (Fossen, 2011). Due to the low speed and the 3 DOF considered, a model describing the kinetics is given by

$$\boldsymbol{M}\dot{\boldsymbol{\nu}} + \boldsymbol{D}\boldsymbol{\nu} = \boldsymbol{\tau}_c + \boldsymbol{\tau}_{\text{env}} \tag{3}$$

where $\boldsymbol{M}$ is the matrix of total inertia including added mass, $\boldsymbol{D}$ is the linear damping matrix, $\boldsymbol{\tau}_c$ is the forces exerted by the thrusters and $\boldsymbol{\tau}_{\text{env}}$ is the environmental forces acting on the ship (Fossen, 2011). In this paper, the focus is on maneuvering the ship and for this reason, the environmental forces will be neglected.

Thrusters

Marine vessels can be equipped with a range of different actuators depending on the intended use. These include propellers, water jets, sails and rudders to name a few (Molland et al., 2011). The purpose of the actuator is to produce a controlled force on the vessel to obtain the desired movement. In low speed motion control, a commonly used actuator is the azimuth thruster (Lewandowski, 2004). It comprises of a propeller mounted on a hub able to rotate (azimuth) freely in the horizontal plane. The control forces and moments created by a thruster are dependent on its location and orientation and on the fluid velocity around the propeller, which in turn relate to the velocity of the ship and the speed of the propeller (Whitcomb and Yoerger, 1999). Moreover, some actuators, such as rudders, will create forces by the water ow. Thus, in the general case, a model of the thrusters is

$$\boldsymbol{\tau}_c = \boldsymbol{h}(\boldsymbol{\nu}, \boldsymbol{u})$$

where $\boldsymbol{u}$ is a vector of control signals, such as thruster angles or propeller speeds. For low speed, the velocity dependency is usually neglected and $\boldsymbol{h}$ typically takes the form (Fossen and Johansen, 2006)

$$\boldsymbol{\tau}_c = \boldsymbol{T}(\boldsymbol{\alpha})\boldsymbol{f}(\boldsymbol{n}) \tag{4}$$

where the control signals u have been split into thruster angles $\boldsymbol{\alpha}$ and propeller speeds $\boldsymbol{n}$. Moreover, $\boldsymbol{f}(\boldsymbol{n}) \in \mathbb{R}^M$ is a vector of thrust magnitude for each thruster, and

$$\boldsymbol{T}(\boldsymbol{\alpha}) = [\boldsymbol{t}_1(\alpha_1), \ldots, \boldsymbol{t}_M(\alpha_M)] \quad \in \mathbb{R}^{n\times M}$$

describes the geometry of the thruster configuration. In 3 DOF, the columns of $\boldsymbol{T}(\boldsymbol{\alpha})$ can be described by

$$\boldsymbol{t}_i(\alpha_i) = \begin{bmatrix} \cos\alpha_i \\ \sin\alpha_i \\ l_{x,i}\sin\alpha_i - l_{y,i}\cos\alpha_i \end{bmatrix}, \quad i = 1, \ldots, M \tag{5}$$

where $l_{x,i}$ and $l_{y,i}$ are the moment arms given in the bod-fiyxed coordinate system and α_i describe the orientation, taken positive clock-wise from the body-fixed x-axis.

For low speed motion control, the thrust f_i produced by the i^{th} thruster is assumed to be proportional to the square of the rotational velocity of the propeller. More precisely, under bollard-pull condition (stationary vessel), a model of a symmetrical propeller's steady-state axial thrust f_i of the i^{th} thruster is given by

$$f_i = k_i n_i |n_i|, \quad i = 1, \ldots, M \tag{6}$$

where k_i is a constant and n_i is the rotational speed of the propeller (Whitcomb and Yoerger, 1999). Subsequently, the thrust vector $\boldsymbol{f}(\boldsymbol{n})$ in (4) can be written as

$$\boldsymbol{f}(\boldsymbol{n}) = \begin{bmatrix} f_1(n_1) \\ \vdots \\ f_M(n_M) \end{bmatrix} = \boldsymbol{K} \begin{bmatrix} n_1|n_1| \\ \vdots \\ n_M|n_M| \end{bmatrix} \tag{7}$$

where $\boldsymbol{K} \in \mathbb{R}^{M\times M}$ is a diagonal matrix with k_1, k_2, ..., k_M on the diagonal.

Motion control for ships

The typical application for ships employing the decoupled motion control described in Section 1 is Dynamic Positioning (DP) where the demands on performance and reliability usually are very strict. A typical DP capable ship come equipped with a redundant set of actuators. This means there are several ways of coordinating the actuators to produce the same net control force on the ship. The redundant actuators also put less emphasis on rotating the thrusters since they can be oriented in such a way that it is possible to quickly generate force and torque in any direction. In this paper, the focus is rather on another class of vessels equipped with fewer actuators where the transient behavior is of importance, for instance, low-speed path following for ferries. This imply that the freedom of the possible thrust is limited, since at any point in time there may be only a few, or not any, ways of coordinating the actuators to produce the desired force.

Before we present the proposed combined model predictive controller for thrust allocation and motion control, theory for model predictive control and general description of thrust allocation will be presented.

Model predictive control

Model Predictive Control (MPC) is an advanced control strategy commonly found in the process industry which uses an explicit model of the system to predict the future behavior. This predictive capability allows solving optimal control problems on-line, where tracking error is minimized over a future horizon, possibly subject to constraints on the manipulated inputs and states (Maciejowski, 2002). In continuous-time, the MPC problem can be written as

$$\begin{aligned} \min_{\boldsymbol{u}} \quad & \int_{t_0}^{t_0+T} \|\boldsymbol{x}(t) - \boldsymbol{x}_r(t)\|^2_{\boldsymbol{Q}_x} + \|\boldsymbol{u}(t) - \boldsymbol{u}_r(t)\|^2_{\boldsymbol{Q}_u}\, dt \\ & \qquad + \|\boldsymbol{x}(t_0+T) - \boldsymbol{x}_r(t_0+T)\|^2_{\boldsymbol{R}_x} && \text{(8a)} \\ \text{s.t.} \quad & \boldsymbol{x}(t_0) = \boldsymbol{x}_0 && \text{(8b)} \\ & \dot{\boldsymbol{x}}(t) = \boldsymbol{f}(\boldsymbol{x}(t), \boldsymbol{u}(t)), \quad \forall t \in [t_0, t_0+T] && \text{(8c)} \\ & \boldsymbol{g}(t, \boldsymbol{x}(t), \boldsymbol{u}(t)) \leq 0, \qquad \forall t \in [t_0, t_0+T]. && \text{(8d)} \end{aligned}$$

where $\boldsymbol{Q}_x \geq 0$, $\boldsymbol{Q}_u > 0$, and $\boldsymbol{R}_x \geq 0$ are weight matrices. Moreover, $\boldsymbol{x} \in \mathbb{R}^{n_x}$ is the state vector, $\boldsymbol{u} \in \mathbb{R}^{n_u}$ is the control input, $\boldsymbol{x}_0$ is the current value of the system state, and $\boldsymbol{x}_r$ and $\boldsymbol{u}_r$ are desired reference trajectories for system state and control input, respectively.

To solve the MPC problem (8) using numerical optimization methods, the cost function and differential equations corresponding to the ship dynamical system need to be discretized. At each sampling instant, the current state is used to initialize the problem and the optimization problem is solved over the horizon $[t_0, t_0+T]$. The solution is a sequence of control inputs and only the first element in the sequence $u^\star(t_0)$ is applied to the system. This process is repeated each sample.

Thrust allocation

The objective of the thrust allocation (TA) is to realize the desired control force by coordinating the available thrusters. The more thrusters the ship is equipped with, the more combinations of inputs may be used. The problem is naturally formulated as a constrained optimization problem, where the objective function may be to minimize the total energy consumption and wear and tear of the actuators, while the constraints describe the objective and physical limitations on the actuators (Johansen and Fossen, 2013). A general problem formulation is

$$\min_{\boldsymbol{u},\boldsymbol{s}} \quad p(\boldsymbol{\eta},\boldsymbol{\nu},\boldsymbol{u},\boldsymbol{s},t) \tag{9a}$$
$$\text{s.t.} \quad \boldsymbol{\tau}_c^d - \boldsymbol{h}(\boldsymbol{\eta},\boldsymbol{\nu},\boldsymbol{u},t) = \boldsymbol{s} \tag{9b}$$
$$\boldsymbol{g}(\boldsymbol{\eta},\boldsymbol{\nu},\boldsymbol{u},t) = 0 \tag{9c}$$

where p is some cost function of the states $(\boldsymbol{\eta},\boldsymbol{\nu})$, inputs $\boldsymbol{u} = (\boldsymbol{n},\boldsymbol{\alpha})$, slack variables $\boldsymbol{s}$ and the time t. The constraint (9b) represent the main priority of the thrust allocation but with the addition of $\boldsymbol{s}$ in case it is not feasible. For low speed, the function $\boldsymbol{h}$ is typically represented by the right hand side of (4).

Finding the global minimum of (9) tends to be di cult since the problem, in general, is non-convex (Fossen and Johansen, 2006). Thus, the algorithm may get stuck in local minima. For rotating and asymmetric thrusters, a thruster may end up stuck producing thrust in reverse of its most efficient direction. To mitigate this, the TA algorithm is usually augmented with external logic determining if it is beneficial to rotate the thrusters (Veksler et al., 2016). Note also that the TA algorithm solves an optimal control problem in similar fashion to the MPC controller described above. In a way, (9) is an MPC formulation with a 1-step prediction horizon.

Combined thrust allocation and motion control

Deviating from the traditional structure, formulating two different optimization problems, we now present a single MPC combining the work of both motion control and TA algorithms similar to Veksler et al. (2016).

From (1), (3) and (4), the combined problem of motion control and TA is formulated as

$$\dot{\boldsymbol{\eta}} = \boldsymbol{R}(\psi)\boldsymbol{\nu}, \tag{10a}$$
$$\boldsymbol{M}\dot{\boldsymbol{\nu}} + \boldsymbol{D}\boldsymbol{\nu} = \boldsymbol{T}(\boldsymbol{\alpha})\boldsymbol{f}(\boldsymbol{n}), \tag{10b}$$

with the system states $(\boldsymbol{\eta},\boldsymbol{\nu})$ and control inputs $(\boldsymbol{n},\boldsymbol{\alpha})$. Both inputs $(\boldsymbol{n},\boldsymbol{\alpha})$ are subject to physical constraints. The propeller speeds $\boldsymbol{n}$ are both limited in magnitude and rate while the thruster angles $\boldsymbol{\alpha}$ are only limited in rate. Combining (10) with the constraints, the continuous-time nonlinear optimization problem is formulated as

$$\min_{\dot{\boldsymbol{n}},\dot{\boldsymbol{\alpha}}} \int_0^{T_s N} \big(\|\boldsymbol{\eta}-\boldsymbol{\eta}_r\|^2_{\boldsymbol{Q}_\eta} + \|\boldsymbol{\nu}-\boldsymbol{\nu}_r\|^2_{\boldsymbol{Q}_\nu} + \|\boldsymbol{n}\|^2_{\boldsymbol{Q}_n} + \|\dot{\boldsymbol{\alpha}}\|^2_{\boldsymbol{Q}_{d\alpha}} + \|\dot{\boldsymbol{n}}\|^2_{\boldsymbol{Q}_{dn}}\big)dt + \text{final cost} \tag{11a}$$
$$\text{s.t.} \quad \dot{\boldsymbol{\eta}} = \boldsymbol{R}(\psi)\boldsymbol{\nu} \tag{11b}$$
$$\boldsymbol{M}\dot{\boldsymbol{\nu}} + \boldsymbol{D}\boldsymbol{\nu} = \boldsymbol{T}(\boldsymbol{\alpha})\boldsymbol{f}(\boldsymbol{n}) \tag{11c}$$
$$\underline{\boldsymbol{n}} \leq \boldsymbol{n} \leq \bar{\boldsymbol{n}} \tag{11d}$$
$$|\dot{\boldsymbol{\alpha}}| \leq \bar{\dot{\boldsymbol{\alpha}}} \tag{11e}$$
$$\underline{\dot{\boldsymbol{n}}} \leq \dot{\boldsymbol{n}} \leq \bar{\dot{\boldsymbol{n}}} \tag{11f}$$

where the final cost contains similar terms as the stage cost. The last two terms in the stage cost penalize the rate of the control inputs to reduce fast changes in the inputs, implying wear and tear reduction on the propulsion equipment. The constraints (11b) and (11c) defines kinematic and dynamic equations of the ship, respectively, while (11d)-(11f) constrain the control inputs.

Combining the high-level controller and TA has several advantages compared to having them separate. For instance, instead of finding bounds on and tuning the weights for the virtual control input $\boldsymbol{\tau}_c^d$, the commissioning engineer may instead

Parameter	Thruster 1	Thruster 2
l_x	32 m	-32 m
l_y	0 m	0 m
Turning rate	±7.2 deg/s	±7.2 deg/s
Available thrust	±1.67 MN	±1.67 MN
Allowed propeller speed	±2 RPS	±2 RPS
Allowed propeller acceleration	±0.08 RPS/s	±0.08 RPS/s

Table 1: Parameters for the thruster models

(a) First test case

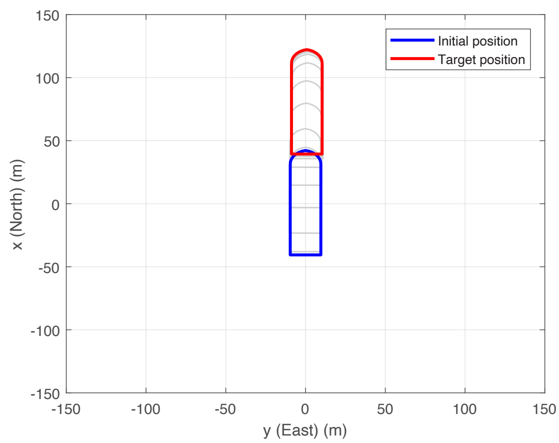

(b) Second test case

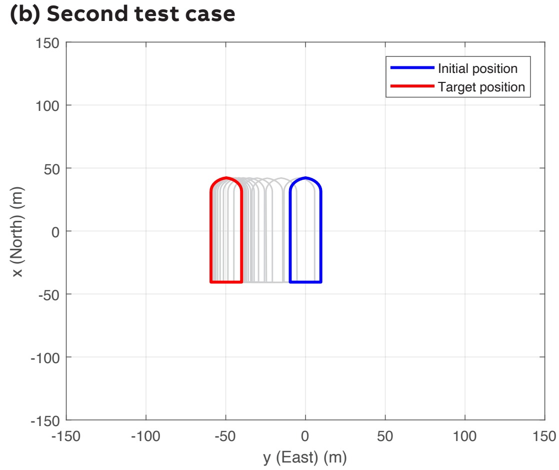

Figure 2: Illustration of the motion in the horizontal plane

Case	Initial position	Initial thruster angles	η_r
1	$[0,\ 0,\ 0]^T$	$[0,\ 0]^T$	$[80,\ 0,\ 0]^T$
2	$[0,\ 0,\ 0]^T$	$[\frac{\pi}{2},\ \frac{\pi}{2}]^T$	$[0,\ -50,\ 0]^T$

Table 2: Summary of test cases and parameters used

use the physical constraints of the thrusters, and tune the weights on $(\boldsymbol{n}, \boldsymbol{\alpha})$ to prioritize among them. Moreover, the trade-o between tracking accuracy and the variation in the actuator inputs is more intuitive since they both appear in the cost function. Further, with a long enough prediction horizon, the MPC should be able to find the long-term benefit of having the thrusters point in the right direction, thus not requiring an external algorithm as mentioned in Section 3.2. Finding the global minimum of (11) is difficult however, and the use of fast end accurate solvers is key.

Implementation

The MPC formulation (11) describe a time-continuous nonlinear optimization problem. As mentioned in Section 3.1, solving it on a computer requires discretizing the problem and using an optimization solver for the resulting problem. Solving a nonlinear problem requires some extra care and, depending on the number of states/inputs and length of the prediction horizon, the optimization problem typically becomes large and time-consuming to solve. In this work, the MPC was developed using the MATLAB interface for the open-source ACADO toolkit (Houska et al., 2011), with the optimization problem solved by QPOASES (Ferreau et al., 2014). The ACADO toolkit allows the user to input the time-continuous formulation, automatically handling the discretization and exporting a fast tailor made solver based on the Real Time Iterations (RTI) scheme. The RTI scheme essentially works by linearizing the problem around the current state estimate and solving one QP in each iteration, thus making it only marginally slower than linear MPC (Gros et al., 2016). The ACADO toolkit does not support the absolute value formulation used in (6). To solve this issue and get a differential function, the absolute value was approximated as

$$|x| \approx \sqrt{x^2 + \varepsilon}$$

Simulation results and discussion

A small ship with two thrusters were chosen to test the proposed motion control system. This configuration was chosen to highlight the potential benefits of the proposed algorithm compared with the issues raised in Section 3.

The simulation model was implemented in Simulink and was based on the supply vessel model available in the MSS hydro toolbox (Fossen and Perez, 2004). This vessel is 82.8 m long, 19.2 m wide and has a displacement of 6360 tons (Fossen and Perez, 2004). The ship model was coupled with a velocity dependent azimuth thruster model. The velocity dependency models water ow over the propeller and rudder effects due to a rudder like geometry of the azimuth thruster body. Two thrusters were used in the simulation, one in the stern and the other in the bow, both mounted on the center line of the vessel. The azimuth model was asymmetric, meaning that it is more efficient to produce thrust with a positive propeller speed. In Table 1, important parameters of the thrusters are found. Note that there was a model mismatch since the velocity dependency was neglected in the MCS.

To counter the asymmetry of the thrusters, the lower bound on $\boldsymbol{n}$ in the MCS was chosen to a fraction of the specified lower bound in Table 1. This made it more beneficial to turn the thruster around when needing to create an opposite force.

The MCS was tested for a wide range of maneuvers. Out of these, the result for two different cases that highlight key features of the proposed solution are presented. Although the proposed solution supports a time-varying reference in velocity and position, it was deliberately chosen to be simple (step change in position) to focus on the behavior of the MCS rather than the trajectory generation. Figure 2 visualizes the motion of the ship for these test cases. Both maneuvers are quite aggressive with a relatively high acceleration and in the upper bound of the low-speed envelope. In both cases, the velocity reference $\boldsymbol{\nu}_r$ was set to zero while a step in position reference $\boldsymbol{\eta}_r$ occurred at t = 8. The differences between the cases are the position reference and the initial thruster orientations, see Table 2. The sample rate was chosen to 2 Hz with the prediction horizon N = 80. Tuning parameters were kept constant through both cases. They were chosen as to produce aggressive maneuvers, while still retaining the general desired behavior. The worst case execution time of the MCS for any test cases was around 0.5 seconds on a laptop with an Intel i7 processor running at 2.9 GHz with 16 GB of RAM.

In the first case seen in Figure 3, the ship is commanded to move to a position in front of it

(a) Position of the vessel along x_n

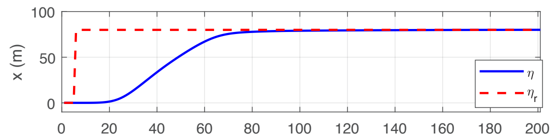

(b) Surge velocity

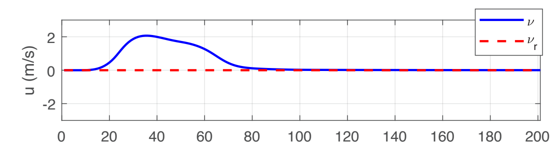

(c) Inputs (n, α) for the thrusters. The angles are wrapped to ±180°.

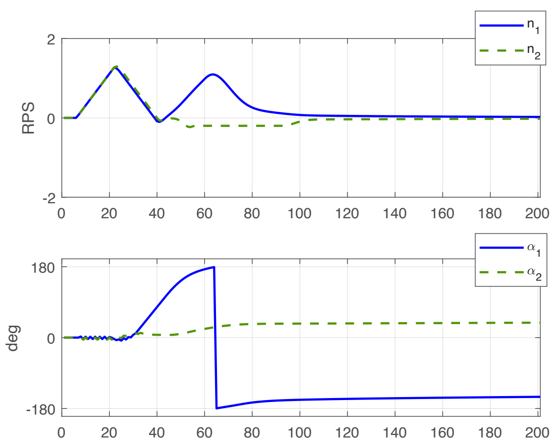

(d) Force exerted on ship τ_c and calculated force to be exerted on the ship using (4), i.e. the internal force in the MCS. The slight mismatch is due to the neglected velocity dependence of the thrusters.

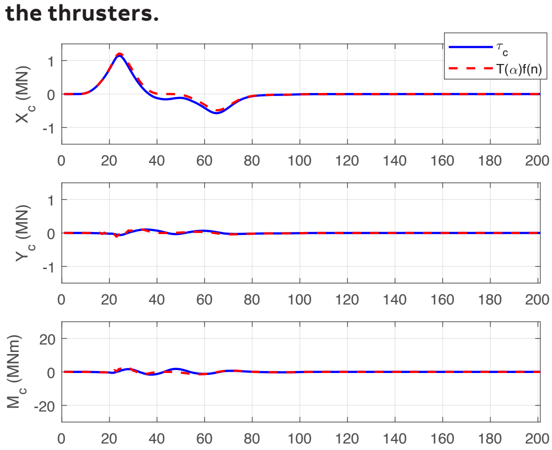

Figure 3: Results of the first test case. The deviation from the reference in the DOF not shown in Figure 3a and Figure 3b were deemed negligible and omitted.

(a) Position of the vessel along x_n

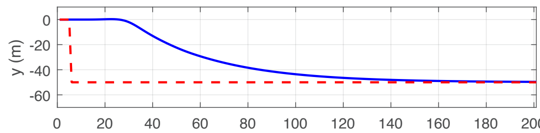

(b) Surge velocity

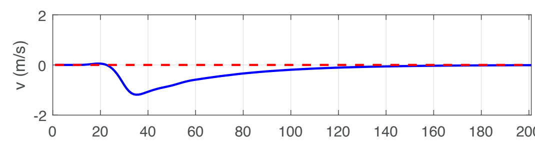

(c) Inputs (n, α) for the thrusters. The angles are wrapped to ±180°.

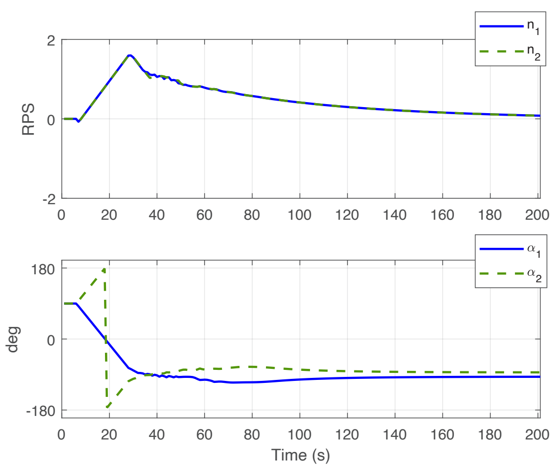

(d) Force exerted on ship τ_c and calculated force to be exerted on the ship using (4), i.e. the internal force in the MCS.

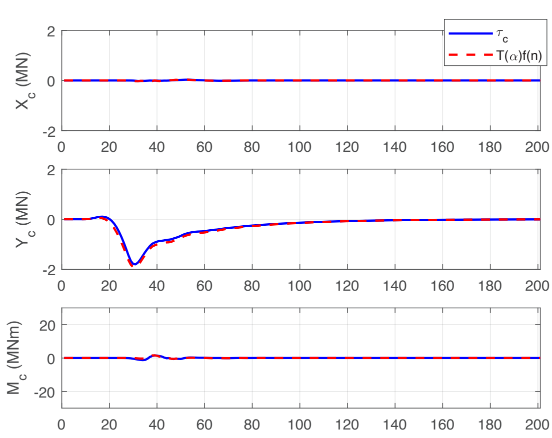

Figure 4: Results of the second test case. The deviation from the reference in the DOF not shown in Figure 4a and Figure 4b were deemed negligible and omitted.

and stop. Thrusters are initially pointing straight forward in the direction of travel. When the step enters, the MCS commands full forward thrust with both thrusters, initially reaching a high speed. After a while, at t = 28, it begins to rotate thruster 2, while simultaneously decreasing n_2 in order to not create too much yaw torque. That is, in anticipation of reaching the target point, the MCS rotates one thruster to maintain in control of the ship. When the thruster is beginning to point in a useful direction, i.e. towards the stern, it accelerates the propeller again to slow down the ship. Meanwhile, the other thrusters reverses slightly to help reduce the speed and correct for yaw- and sway movement. Thus, the MCS manages to overcome the rotation time of the thrusters and stop the ship in time.

This kind of thruster control would be di cult to achieve using a traditional hierarchy for the MCS since the TA, in its usual form only tries to achieve the current desired force. In cases such as this, where the maneuver is aggressive and the ship is not able to generate force in all DOF simultaneously, the performance will most likely degrade with the traditional setup. A force mismatch will occur between what the high-level controller wants and what the TA can deliver, due to the rotation time of the thrusters which is unknown to the high-level controller. Thus, one would have to rely on slower and more conservative maneuvers, where there is room for a deviation between the desired and actual force. This could for instance be achieved by a careful and conservative tuning of the motion controller, or by generating a trajectory known to be achievable.

The second test case can be seen in Figure 4. The ship now has to move in a negative y_b-direction while the thrusters initially are pointing straight in positive y_b. The MCS completes this maneuver by first rotating the thrusters 180 degrees to allow for positive RPM. Since the MPC has knowledge on the physical limitations of the thrusters it will only require a feasible force. In this case, the traditional solution with a one-step TA might get stuck reversing the thrusters or request a large force that is not achievable with the current state of the thrusters. Since the TA only tries to fulfill the current desired force, it will not take into account the long term benefit of having the thrusters point in the right direction.

Conclusion

In this paper, a combined MPC for motion control and thruster allocation was presented. The problem was formulated with a low-speed ship and thruster model and the aim was to improve maneuvering behavior. The MPC problem was implemented with the ACADO toolkit with the RTI scheme. The test result and execution time on the test computer indicate that this problem can be run in real-time on today's hardware.

It appears that the combined MPC offers improvements in control performance compared to capabilities of the traditional decoupled approaches. The combined MPC has full knowledge on the state and limitations of the thrusters and is able to coordinate them more efficiently throughout the control horizon. It accounts for the delay caused by the rotation time of the thrusters when planning the motion. This makes it more robust to different tuning and aggressive maneuvers. Although the behavior was satisfactory, it is di cult to tell if this is the optimal behavior with respect to the objective. Convergence of the solver is not guaranteed and care should be taken to ensure that it does not get stuck in local minima. In the current implementation, the thruster model was kept simple. Future work includes extension of the thruster model to include velocity dependencies and asymmetry. Moreover, the power of the thruster is typically proportional to the cube of the engine speed and more work should be spent on understanding the impact of the quadratic cost function. Finally, the impact of environmental disturbances should be considered in future developments to complement the maneuvering behavior.

—
A. Bärlund, J. Linder, H.R. Feyzmahdavian, M. Lundh and K. Tervo. Nonlinear MPC for combined motion control and thrust allocation of ships. In Proceedings of the 21st IFAC World Congress, Berlin, Germany, July 2020

—
References

Ferreau, H., Kirches, C., Potschka, A., Bock, H., and Diehl, M. (2014). qpOASES: A parametric active-set algorithm for quadratic programming. Mathematical Programming Computation, 6(4), 327 363.

Fossen, T.I. and Johansen, T.A. (2006). A survey of control allocation methods for ships and underwater vehicles. In 2006 14th Mediterranean Conference on Control and Automation, 1 6. doi:10.1109/MED.2006. 328749.

Fossen, T.I. and Perez, T. (2004). Marine systems simulator (mss). URL https://github.com/cybergalactic/MSS.

Fossen, T.I. (2011). Handbook of Marine Craft Hydrodynamics and Motion Control. Wiley, first edition.

Gros, S., Zanon, M., Quirynen, R., Bemporad, A., and Diehl, M. (2016). From linear to nonlinear mpc: bridging the gap via the real-time iteration. International Journal of Control, 0(0), 1 19. doi:10.1080/00207179. 2016.1222553.

Houska, B., Ferreau, H., and Diehl, M. (2011). ACADO Toolkit An Open Source Framework for Automatic Control and Dynamic Optimization. Optimal Control Applications and Methods, 32(3), 298 312.

Hvamb, O.G. (2001). A new concept for fuel tight dp control. In Dynamic Positioning Conference.

Johansen, T.A. and Fossen, T.I. (2013). Control allocation – a survey. Automatica, 49(5), 1087 1103. doi:10.1016/ j.automatica.2013.01.035.

Lewandowski, E.M. (2004). The Dynamics of Marine Craft. WORLD SCIENTIFIC. doi:10.1142/4815.

Li, Z., Sun, J., and Oh, S. (2009). Path following for marine surface vessels with rudder and roll constraints: An mpc approach. 3611 3616.

Maciejowski, J.M. (2002). Predictive Control with Constraints. Prentice Hall.

Molland, A.F., Turnock, S.R., and Hudson, D.A. (2011). Ship Resistance and Propulsion. Cambridge, first edition.

Perez, T. (2005). Ship Motion Control. Springer, first edition.

Skjong, S. and Pedersen, E. (2017). Nonangular mpc-based thrust allocation algorithm for marine vessels a study of optimal thruster commands. IEEE Transactions on Transportation Electrification, 3(3), 792 807. doi:10.1109/TTE.2017.2688183.

Sørensen, A.J. (2011). A survey of dynamic positioning control systems. Annual Reviews in Control, 35(1), 123 136. doi:10.1016/j. arcontrol.2011.03.008.

Sørensen, A.J. (2012). Marine control systems propulsion and motion control of ships and ocean structures lecture notes.

Sotnikova, M.V. and Veremey, E.I. (2013). Dynamic positioning based on nonlinear mpc. IFAC Proceedings Volumes, 46(33), 37 42. doi:10.3182/20130918-4-JP-3022. 00058. 9th IFAC Conference on Control Applications in Marine Systems.

Veksler, A., Johansen, T.A., Borrelli, F., and Realfsen, B. (2016). Dynamic positioning with model predictive control. IEEE Transactions on Control Systems Technology, 24(4), 1340 1353. doi:10.1109/ TCST.2015. 2497280.

Wahl, A. and Gilles, E.D. (1998). Track-keeping on waterways using model predictive control. IFAC Proceedings Volumes, 31(30), 149 154.

Whitcomb, L.L. and Yoerger, D.R. (1999). Development, comparison, and preliminary experimental validation of nonlinear dynamic thruster models. IEEE Journal of Oceanic Engineering, 24(4), 481 494. doi:10.1109/48. 809270.

Zheng, H., Negenborn, R.R., and Lodewijks, G. (2014). Trajectory tracking of autonomous vessels using model predictive control. IFAC Proceedings Volumes. 19th IFAC World Congress, Cape Town, South Africa.